Integrative oncology using the *viscum album* therapy improves quality of life in a dog diagnosed with oral fibrosarcoma - case report

Oncologia integrativa por meio da terapia *viscum album* melhora a qualidade de vida em um cão diagnosticado com fibrossarcoma oral - relato de caso

DOI:10.34117/bjdv8n3-149

Recebimento dos originais: 14/02/2022
Aceitação para publicação: 12/03/2022

Ana Catarina Viana Valle
Doutora em Genética & Biotecnologia
Instituição: Instituto IDIS/Lamasson, Ribeirão Preto, Brasil
Endereço: Ribeirao Preto, SP, Brazil
E-mail: dranacatarina@gmail.com

Aloisio Cunha de Carvalho
Doutor em Patologia Ambiental
Instituição: Instituto IDIS/Lamasson, Ribeirão Preto, Brasil
Endereço: Ribeirao Preto, SP, Brazil
E-mail: acarvalhovet@gmail.com

ABSTRACT
Cancer in dogs and cats comprises a complex process with several variables. For this reason, its treatment is difficult and often does not offer many benefits to patients. Oral fibrosarcoma is a relatively common neoplasm in veterinary oncology, and it is among the three most frequent neoplasm in canine species. Conventional treatment is, in general, surgical followed by chemotherapy and/or radiotherapy. However, such therapy does not contemplate the cure or even the patients' quality of life. Within this context, integrative therapies arise to offer a better quality of life and longevity to cancer patients, valuing their welfare. Homeopathy has gained emphasis in this area, offering patients relief and quality of life. It is used as a single therapy and/or combined with conventional treatments and can reduce the side effects caused by the latter. This study aimed to report the integrative treatment of a canine patient diagnosed with oral fibrosarcoma using the *Viscum album* therapy, injectable homeopathy, chromotherapy, among others, which provided quality and survival of 27 months.

Keywords: mistletoe, cancer, dog, complementary therapy.

RESUMO
O câncer em cães e gatos compreende um processo complexo com diversas variáveis. Por esse motivo, seu tratamento é difícil e muitas vezes não oferece tantos benefícios aos pacientes. O fibrossarcoma oral é uma neoplasia relativamente comum na oncologia veterinária, estando entre as três neoplasias mais frequentes na espécie canina. O tratamento convencional é, em geral, cirúrgico seguido de quimioterapia e/ou radioterapia. No entanto, tal terapia não contempla a cura ou mesmo a melhoria de qualidade de vida dos pacientes. Dentro desse contexto, as terapias integrativas surgem para oferecer com esse objetivo e oferecendo longevidade aos pacientes com câncer,

valorizando o seu bem-estar. A homeopatia tem ganhado destaque nesta área, proporcionando aos pacientes alívio e qualidade de vida, podendo ser administrada como terapia única e/ou combinado com tratamentos convencionais, reduzindo os efeitos colaterais causados por estes últimos. Este trabalho teve como objetivo relatar o tratamento integrativo de um paciente canino diagnosticado com fibrossarcoma oral utilizando a terapia *Viscum album*, homeopatia injetável, cromoterapia, entre outros, que proporcionou qualidade e sobrevida de 27 meses.

Palavras-chave: viscum, câncer, cão, terapia complementar.

1 INTRODUCTION

Fibrosarcomas are malignant mesenchymal neoplasms [1]. The etiology of this tumor is related to vaccinations, radiation, genetic factors, and chemical carcinogens [2]. According to recent data, there is a breed predisposition to canine fibrosarcoma [3], [4], and the most affected breeds are the Swiss mountain dog, the Rottweiler, the Retriever (Golden and Labrador), the Doberman, the Boxer, the Shepherd, the Terrier, the Pinscher, and the Gordon Setter [3-5]. Based on the contrasting data available, it seems there is no sex predisposition [3-5]. It is commonly reported in middle-aged to elderly dogs, ranging between 7 and 12 years old [5], [6]. It accounts for 7.5 to 25% of all oral cavity cancer cases [6], and it is the third most common neoplasm found in the oral cavity of dogs. Fibrosarcoma accounts for 12.9% of all neoformations and 2.3% to 2.6% of malignant tumors [7].

It is considered locally invasive and may invade adjacent bone tissue and make it difficult to distinguish between primary and secondary neoplasms. In contrast, it is little metastatic (only 20 to 25% of the cases), and when it occurs, metastasis usually affects the lungs and liver via the hematogenous route [2]. Affected animals may experience pain at the site of the neoplasm, and when there is bone involvement, clinical signs include reluctance to support the limb, lameness, and pathological fracture. The clinical signs are most severe when metastasis is present, including dyspnea and jaundice in pulmonary and hepatic cases, respectively [8].

The definitive diagnosis is made by histopathological examination [2]. Radical surgical excision of the mass at the site of origin is indicated as the treatment of choice. Safety margins of 3 to 5 cm are used based on the biological behavior, histopathological characteristics, and tumor stage. Amputation is the indicated treatment when it is located in the limbs. As this type of neoplasm has an infiltrative growth, mass removal may not be effective in some situations [9], [10]. Therefore, recurrences may occur (30 to 70%

rate of occurrence), on average, six months after the procedure. For this reason, it is indicated the association of radiotherapy and/or chemotherapy with surgical treatment [9], [10]. The prognosis of patients with fibrosarcoma is favorable when the tumor is small, with no metastasis, and free surgical margins. However, the prognosis is reserved when it exceeds 8 cm in diameter and/or metastasis is present [10].

Conventional cancer treatments do not cure the disease or improve patients' quality of life. For this reason, it is necessary to search for unique or even complementary treatments that mitigate the side effects caused by conventional therapies. In this context, integrative treatments emerge, and integrative oncology stands out to provide a better quality of life for these patients, mainly through *Viscum album* therapy [11].

Viscum album is a plant of European origin with outstanding immunomodulatory activity for the host and selective cytotoxic activity for the tumor [12]. Medicines derived from this plant can be dispensed according to the Anthroposophical Medicine precepts or the homeopathic pharmacopeia for the same purpose [13]. Several authors have reported good results for cancer treatment with this therapy [13].

This study aimed to report the treatment of a 10-year-old dog, Golden retriever breed, diagnosed with oral fibrosarcoma. The patient was treated by integrative oncology with an emphasis on the *Viscum album* therapy, with no maxilla amputation, and had 27-month survival.

2 CASE REPORT

A 10-year-old Golden Retriever, male, neutered, was seen at NaturalPet, Brasilia, Brazil, in 2018. The animal had a diagnosis of oral fibrosarcoma located in the medial portion of the left mandible, at the level of the premolar tooth, and with two months of apparent evolution. The tumor had already been removed 40 days prior to the appointment at Naturalpet Clinic, and it was recommended a unilateral maxillectomy by the Veterinarian in charge of the case. However, the owners refused to perform the procedure and sought the Complementary Medicine service at Naturalpet Clinic. On physical examination, the animal was cheerful, with normal colored mucosa, TPC 2", cardiac and respiratory auscultation within the normal range for age and species, lymph nodes within the normal range. Upon inspection of the oral cavity, an inflammatory lesion was observed in the peri-gingival region of the lower left first molar. A blood sample was collected for complete blood count and biochemical measurements. The following injectable medicines were prescribed: *Viscum album* D3, D6, D9, D12, and D30

(Injectcenter®), *Mercurius solubilis* D35 (Injectcenter®), *Apis melifera* D6 (Injectcenter®), and *Chelidonium majus* D35 (Injectcenter®), subcutaneously, combined in the same syringe, once a day, for 90 days. *Phosphorus* 30CH, three drops, once a day, for 30 days, was also orally prescribed. In addition, the patient was fed a ketogenic diet prescribed by another colleague. Furthermore, the animal should return to the clinic once a week for intravenous application of one ampoule of *Viscum album* D3 (Injectcenter®), associated with autohemotherapy. Autohemotherapy was performed by withdrawing 2 mL of blood from the jugular vein followed by its subcutaneous application back in the patient. *Viscum album* (Injectcenter®) was also subcutaneously applied using an insulin syringe and hypodermic needle (45X13) in the site where the fibrosarcoma was removed and diagnosed.

3 RESULTS

After 15 days of the treatment initiation, the patient was cheerful. According to its owner, there was an improvement in appetite, overall disposition, and sleep along with a reduction in the state of fatigue previously presented. As a consequence, the animal restarted playing with its toys. The blood sample collected for blood count and biochemical tests resulted in suitable parameters (Table 1 - 8-Nov-18). The first computed tomography (CT), performed in October 2018 (Figure 1), showed images suggestive of an amorphous and isodense neoformation located in the lateral region of the third left premolar tooth, measuring about 0.78 cm high x 0.4 cm wide x 0.5 cm long (Figure 1B). The cranial vault showed preserved conformity and bone density. Lateral, third, and fourth ventricles had typical morphological characteristics for the patient's age (Figure 1C). No further detectable changes. Thorax - the bone structures of the thoracic framework were preserved, with no metastatic pulmonary nodules. Topography of sternal, mediastinal, and tracheobronchial lymph nodes with no detectable changes (Figure 1D). The cardiac silhouette was within the normal limits. Normal posterior elements. No further noteworthy changes. Abdomen - the liver, pancreas, and adrenal glands had normal dimensions and contours and no focal lesions. The gallbladder presented sedimentary isodense content (Figure 1A). The spleen had regular volume and contours, heterogeneous enhancement, presence of multiple nodules throughout the splenic parenchyma, the largest measuring approximately 0.6 cm in diameter (Figures 1E

and F). Presence of a hyperdense structure inside the urinary bladder. Normal prostate and posterior elements. No further noteworthy changes.

Figure 1: Indicated by the green arrows. A) Gallbladder presents sedimentary isodense content. B and C) Images suggestive of an amorphous and isodense neoformation in the lateral region of the third left premolar tooth measuring approximately 0.78 cm in height x 0.4 cm in width x 0.5 cm in length. D) Thorax within normality. E and F) Spleen with multiple hyper-uptake nodules randomly distributed throughout the splenic parenchyma, the largest nodule measuring about 0.6 cm in diameter.

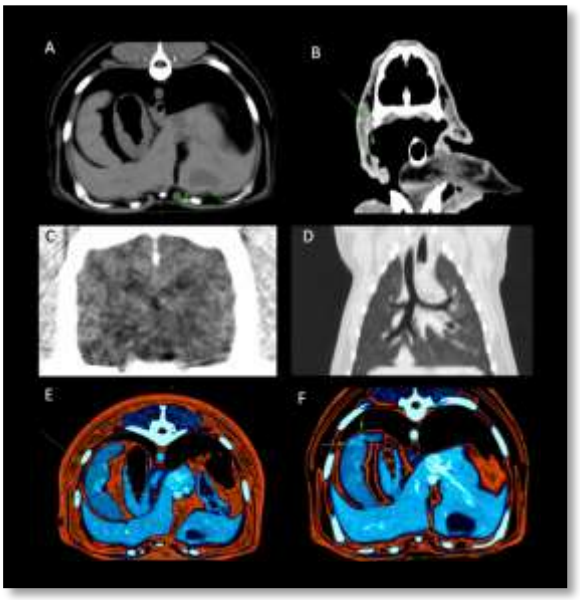

Table 1: Blood count and biochemical measurements performed during the follow-up period of the present report.

	08-Nov-18	*06-Dec-18*	*16-Jan-19*	*25-Apr-19*	*01-Aug-19*	*24-Oct-19*	*11-Jan-20*	*01-Sept-20*	*01-Oct-20*	*07-Oct-20*	*10-Oct-20*
Red blood cells (µL)	5,920,000	6,140,000	5,910,000	5,910,000	5,720,000	5,740,000	5,830,000	6,610,000	5,490,000	5,490,000	3,240,000
Hemoglobin (g/dL)	14.3	13.8	14	13.5	13.6	13.2	13.2	15.1	12.6	13.7	7.5
Hematocrit (%)	39.9	41.9	39.5	39	38.2	38.9	37.5	42.6	35.7	40.7	23.2
MCV (fL)	67.4	68.24	66.84	65.99	66.78	67.77	64.32	64.9	65.03	68.52	71.9
MCHC (g/dL)	35.84	32.94	35.44	34.62	35.6	33.93	35.2	35.2	35.29	33.66	32.3
Leukocytes (µL)	7,100	6,400	6,700	6,300	6,200	11,400	6,900	6,400	17,700	17,300	18,000
Basophils (µL)	0	0	0	0	0	0	0	0	0	0	0
Eosinophils (µL)	1,136	0	536	819	62	456	345	128	708	346	0
IN* (µL)	0	0	0	0	0	0	0	0	177	0	0

SN* (µL)	4,828	4,416	4,824	3,653	5,084	9,120	5,865	4,416	15,222	14,787	97
Lymphocytes (µL)	1,136	1,855	1,340	1,764	992	1,482	690	1,855	1,456	519	1
Monocytes (µL)	0	128	0	63	62	342	0	0	177	1,557	2
Platelets (µL)	537,000	345,00	417,000	419,000	416,000	420,000	363,000	376,000	325,000	287,000	58,000
TPP* (g/dL)	8	7.8	7.6	8	8	8.4	7.2	7.8	7.4	7.2	4.5
ALT (U/L)	**	31	33	49	59	103	48	40	58	**	115
Cholesterol (mg/dL)	**	**	**	**	**	273	248	**	**	**	**
Creatinine (mg/dL)	**	1.22	0.88	0.57	0.71	0.67	0.75	0.92	6.14	6.4	2.7
AP* (U/L)	**	28	44	40	20	64	22	61	150	**	444
Phosphorus (mg/dL)	**	4.94	**	**	**	4.18	4.15	**	12.49	8.64	5.4
Potassium (mmol/L)	**	4.97	**	**	**	4.14	4.67	**	4.25	**	4.11
Urea (mg/dL)	**	40	43	43	43	38	38	39	383	105	139
Triglycerides (mg/dL)	**	**	**	**	**	**	64	**	**	**	**

*PPT – total plasma protein; SN – segmented neutrophils; IN – immature neutrophils; AP - alkaline phosphatase

After CT, a new surgical procedure was performed to remove the affected premolar tooth. The anterior and posterior teeth to the affected premolar were also removed. Bone scraping and cauterization at 50 ^{o}C of the affected region were performed. A biopsy was performed, and the tissue sample was referred for histopathological analysis. The results showed about 70-90% of the fragments with neoplastic cells (Figure 2). The lesion was hypercellular, infiltrative, well-demarcated, not encapsulated, expanding and replacing the submucosa. The neoplastic cells were arranged in random bundles, mostly cohesive, supported by a moderate fibrovascular stroma. These cells were fusiform, with moderately distinct edges and moderate eosinophilic and homogeneous cytoplasm. The nucleus was large and elongated, single or double, with loose chromatin and evident nucleoli (single or double). It had anisocytosis, moderate anisokaryosis, and two mitoses per ten high power fields (400X). The vessels were free of neoplastic cells, but the margins were compromised. Areas with discrete eosinophilic and amorphous

material deposition and cellular debris (necrosis), neutrophils, and macrophages were observed. The histopathological diagnosis was fibrosarcoma (70-90%).

Figure 2: Malignant proliferation of fibroblasts represented by the black star.

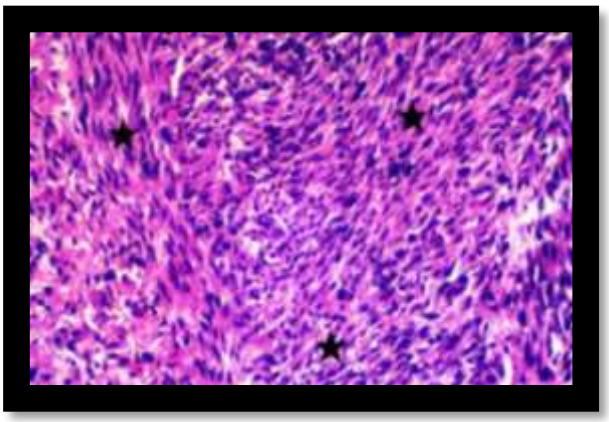

The treatment protocol remained the same after the surgical procedure. In December 2018, additional exams were performed (Table 1 - Dec-18), demonstrating stability in the blood count and biochemical measurements compared to the last exam performed in November 2018. The clinical condition of the animal remained stable from December to April (Table 1 - Dec-18, Jan-19, and Apr-19). In May 2019, the patient underwent a new CT to monitor the evolution of the case.

CT performed in May 2019 (Figure 3): Skull - the cranial vault had preserved conformity and bone density (Figure 3C). The images suggested the partial absence of the left maxilla and teeth 205, 206, 207, and 208. Lateral, third, and fourth ventricles had normal morphological and attenuation characteristics for the patient's age. Bone structures were preserved, and no signs compatible with internal ou media otitis were characterized. Abdomen - liver with typical volume, regular contours, and heterogeneous contrast enhancement. Presence of a low-uptake contrast nodule (Figure 3B) in the left medial lobe topography, with approximately 1.1 cm in diameter. The pancreas and adrenal glands had typical dimensions and contours, homogeneous attenuation, uniform enhancement, no focal lesions. The spleen showed increased volume, regular contours, and heterogeneous contrast enhancement. Presence of multiple hyper-uptake nodules (Figure 3A) distributed in the parenchyma, more evident in the dorsal portion, the largest measuring approximately 1.2 cm in diameter. The kidneys, abdominal aorta, caudal vena cava, and portal vein were normal. Intestinal loops were tomographically normal. The urinary vesicle and prostate were within normal limits. Normal posterior elements.

Isoattenuating content with characteristics of intervertebral disc protrusion between the L7-S1 vertebrae (Figure 3D), central. Thorax - the bone structures of the thoracic framework were preserved, showing no signs of fractures and/or bone lysis, nor the loss of their morphological characteristics and conformations. No metastatic pulmonary nodules were detected. The cardiac silhouette, thoracic aorta, and cranial and caudal vena cava were normal.

After the CT performed in May 2019, the treatment protocol was modified with the addition of subcutaneous applications of *Chelidonium majus* D35 (Injectcenter®) and *Taraxacum officinalis* D35 (Injectcenter®), one ampoule of each, on alternate days; and 20 minutes of chromotherapy once a week (blue light, with crystal light refraction, with a frequency of 700 Hertz, located at the height of the liver). *Viscum album* D2 (Injectcenter®) was also administered twice a week, intravenously, replacing the once-a-week application. The animal continued to be followed up by another colleague regarding food care and remained on a ketogenic diet. The treatment continued until August 2019, with blood sample collection (Table 1 - Aug-19) for follow-up. An additional CT was performed as per the owner's request. The blood count and the biochemical measurements remained within the normal range compared to the last exam performed in May 2019.

CT performed in August 2019: Skull - images suggestive of partial absence of the left maxilla, as well as teeth 205, 206, 207, and 208 (Figure 4). Preserved conformity and bone density of the cranial vault. Absence of signs of meningeal thickening, no abnormal contrast uptake, no evidence of meningitis. Ear canals were normally aerated, and bone structures were preserved. Posterior elements were normal, with no further detectable changes. Thorax - the bone structures of the thoracic framework were preserved. No metastatic pulmonary nodules were detected. Cervical and thoracic segments of the trachea were pervious, with preserved anatomical paths and no alteration in their luminal calibers. The cardiac silhouette, thoracic aorta, and cranial and caudal vena cava were normal. Normal posterior elements. No further noteworthy changes. Abdomen - the stomach was slightly distended with the presence of gas and liquid content inside. The liver had regular volume and contours. However, it presented heterogeneous enhancement and a low-uptake contrast nodule in the left medial lobe, approximately 0.68 cm in diameter. The pancreas and adrenal glands were normal. Spleen had increased volume, regular contours, and heterogeneous contrast enhancement. Presence of multiple hyper-uptake nodules randomly distributed throughout the splenic parenchyma, the

largest measuring approximately 1.08 cm in diameter. The kidneys, abdominal aorta, caudal vena cava, and portal vein were normal. The intestinal loops and prostate were within the normal range. Isoattenuating content with intervertebral disc protrusion between the L7-S1 vertebrae, central, measuring approximately 158 HU* (Hounsfield Unit), characterizing the intervertebral disc material. It occupied about 70% of the vertebral canal, thus compressing the innervations of the spinal cord. Normal posterior elements. No further noteworthy changes.

Figure 3: A) Spleen with multiple hyper-uptake nodules randomly distributed throughout the splenic parenchyma. B) Liver with a nodule. C) Skull with normal morphological and attenuation characteristics. D) Lumbosacral vertebra hernia.

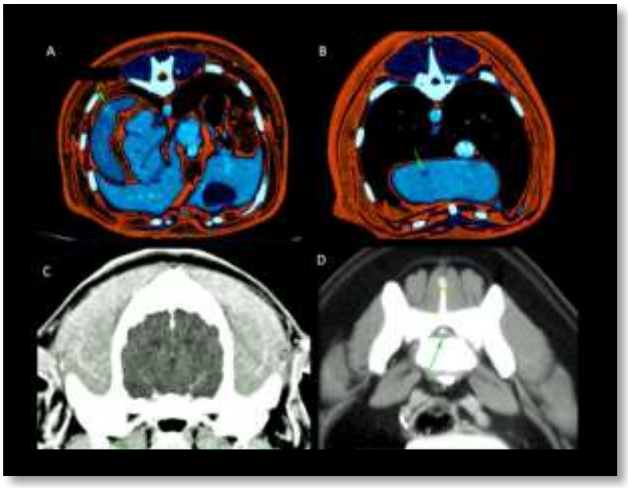

Figure 4: Images suggestive of partial absence of the left maxilla and teeth 205, 206, 207, and 208.

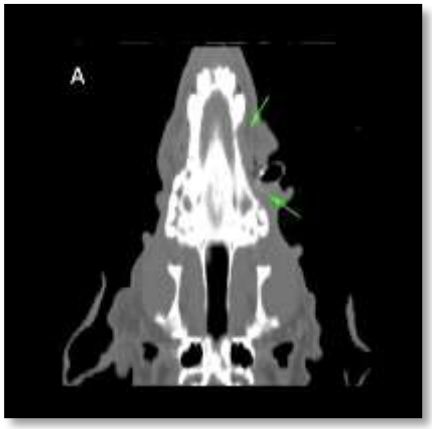

The treatment protocol was not modified after the CT performed in August 2019. The patient remained clinically stable, with no further change in his clinical behavior. New blood count and biochemical measurements were carried out in October 2019 (Table

1 - Oct-19), showing a slight alteration in the liver enzymes and a significant alteration in the total leukocyte count.

In January 2020, a blood sample was collected for an additional blood count and biochemical measurements. The results were within the normal range (Table 1 - Jan-20). The animal was clinically well, but a new CT was performed for follow-up.

CT performed in January 2020: Skull - absence of the first upper right incisor tooth and the upper left premolars (101, 205, 206, 207, and 208). Preserved conformity and bone density of the cranial vault. Absence of hemorrhagic collections, cysts, abscesses, or intracranial neoplasms. The left auditory canal was normally aerated. Preserved bone structures, no signs compatible with media or internal otitis. Presence of isodense content within the right horizontal canal, close to the tympanic membrane. The tympanic bulla was preserved. The left medial retropharyngeal lymph node presented a slight increase in its volume, regular contours, and heterogeneous contrast enhancement, evidencing an oval, low-uptake, well-delimited nodule, measuring approximately 0.2 cm in diameter. The posterior elements were normal. No further changes were detected. Thorax - preserved bone structures of the thoracic framework. Images suggestive of bilateral axillary lymph node enlargement. No metastatic pulmonary nodules were detectable. The cardiac silhouette, thoracic aorta, and cranial and caudal vena cava were normal. An oval, isodense, and hyper-uptake nodule was visualized in the subcutaneous tissue of the left ventrolateral region of the chest at the level of the eleventh rib. It had well-defined limits and measured approximately 1.4 cm in diameter. Posterior elements were normal. No further noteworthy changes. Abdomen - the liver had regular volume and contours, heterogeneous contrast enhancement, and presented a low-uptake nodule in the left medial lobe, measuring approximately 1.18 cm in diameter (Figure 5). The pancreas and adrenal glands were normal. Spleen had increased volume, regular contours, and heterogeneous contrast enhancement. Presence of multiple hyper-uptake nodules with poorly defined limits distributed in the splenic parenchyma, the largest measuring about 1.7 cm in diameter and located in the head of the spleen. The kidneys, abdominal aorta, caudal vena cava, and portal vein were normal. The intestinal loops and urinary bladder were within normal limits. Images suggesting increased volume of iliac and bilateral inguinal lymph nodes. The prostate was within the normality patterns. Normal posterior elements. No further noteworthy changes.

Figure 5: A) Presence of multiple nodules in the spleen. B) Presence of a single nodule in the liver. C) Presence of nodule located in the head of the spleen. D) Lungs with no alteration. E) Presence of disc protrusion in L7-S1.

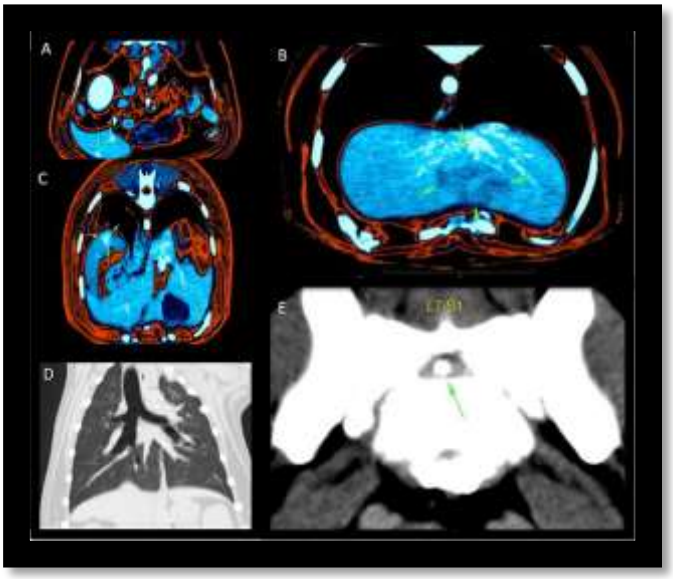

The treatment protocol was modified right after the result of this CT. The patient remained clinically stable, with no further change in his clinical behavior. Fermented *Viscum album* P D3 (Injectcenter®/Iscador®) was added once a week, subcutaneously, and twice a week, intravenously. The *Viscum album* in combinations (Injectcenter®) was maintained once a day, subcutaneously, four times a week. The remaining medications were not altered. However, chromotherapy was suspended, and rectal ozone therapy was started once a week.

In March 2020, the owners reported gingival growth superior to the right canine (Figure 6). Dental prophylaxis was performed to remove the fragment, and the histopathological analysis resulted in the diagnosis of epulis.

Figure 6: Gingival mass in the right canine.

An additional CT was performed in July 2020 (Figure 7): Skull - presence of an oval, expansive, and infiltrative neoformation, with well-defined limits and contrast hyper-uptake in the left maxilla (Figure 7B), at the level of the upper premolars (it invaded the left nasal cavity in the ventral nasal meatus topography; Figures 7C and D). The neoformation measured about 2.58 cm in height x 2.48 cm in width x 3.30 cm in length (Figure 7E). Absence of upper teeth, suggestive of being the first and third right incisors, right canine, and left premolars (teeth 101, 103, 104, 205, 206, 207, and 208). Bone lysis of the alveolar processes from the left premolar teeth, left maxilla, and palatine process of the left maxilla were observed (Figure 7A). Presence of isodense content in the direct external auditory canal, close to the tympanic membrane, in addition to intramural mineralization foci in a bilateral horizontal canal. Preserved bone strutures. Left medial retropharyngeal lymph node with slightly increased volume, regular contours, and heterogeneous contrast enhancement, evidencing an oval, low-uptake, well-delimited nodule measuring approximately 0.2 cm in diameter. Normal posterior elements. No further changes were detected. Thorax - no signs of fractures and/or bone lysis, nor the loss of their morphological characteristics and conformations. No metastatic pulmonary nodules were detected. The cardiac silhouette, thoracic aorta, and cranial and caudal vena cava were normal. Normal posterior elements. No noteworthy changes. Abdomen - liver with preserved volume, regular contours, and heterogeneous contrast enhancement. Presence of a low-uptake nodule in the left medial lobe, with defined limits, measuring approximately 1.20 cm in height x 1.95 cm in width x 0.98 cm in length (Figure 8B). An amorphous area with poorly defined limits was also visualized. It had heterogeneous contrast uptake, with low-uptake and hyper-uptake areas, was located in the liver quadrate lobe topography, and measured about 4.09 cm in height x 5.06 cm in width x 5.19 cm in length. The spleen had increased volume, rounded edges, heterogeneous contrast enhancement, and multiple hyper-uptake nodules with poorly defined limits distributed throughout the splenic parenchyma. The largest nodule was in the head of the spleen and measured approximately 1.80 cm in diameter (Figure 8C). The pancreas, adrenal glands, kidneys, abdominal aorta, caudal vena cava, and portal vein were normal. The urinary bladder had no abnormalities. Abdominal lymph nodes were enlarged (Figure 8A). The prostate was within the tomographic standards. A well-delimited, oval, isodense, subcutaneous nodule was located in the left ventrolateral region of the cranial abdomen, at the level of the ninth rib, measuring approximately 1.4 cm in diameter. Hyperattenuating content with characteristics of intervertebral disc protrusion between

the L7-S1 vertebrae, center-lateral to the left, measuring approximately 258 HU* (Hounsfield Unit), consistent with mineralized material from the intervertebral disc, occupying about 70% of the vertebral canal, thus compressing the spinal cord innervations, leading to partial neural occlusion of the bilateral foramina. Normal posterior elements. No further noteworthy changes.

Figure 7: A) Bone lysis of the alveolar processes from the left premolar teeth, left maxilla, and palatine process of the left maxilla. B, C, D) Presence of an oval, expansive, infiltrating neoformation, with well-defined limits, located in the left maxilla at the level of upper premolars, invading the left nasal cavity, in the topography of the ventral nasal meatus. E) Tumor involvement of the left maxilla.

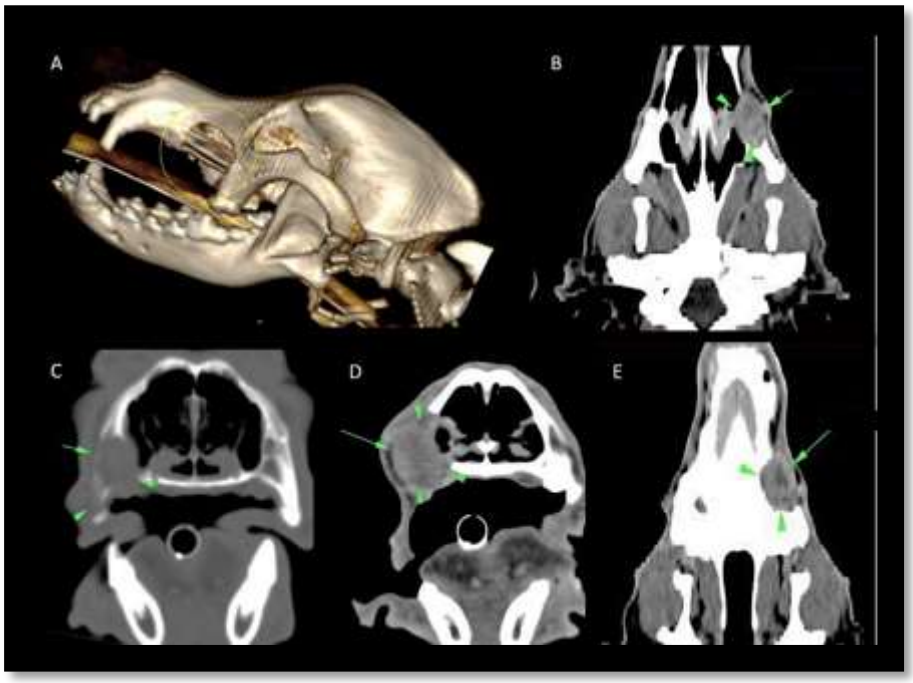

Figure 8: A) Enlarged abdominal lymph nodes. B) Liver - Presence of a low-uptake nodule in the left medial lobe, with defined limits, measuring approximately 1.20 cm in height x 1.95 cm in width x 0.98 cm in length. Presence of an amorphous area with poorly defined limits, heterogeneous contrast uptake comprising low-uptake and hyper-uptake areas, located in the liver quadrate lobe topography.

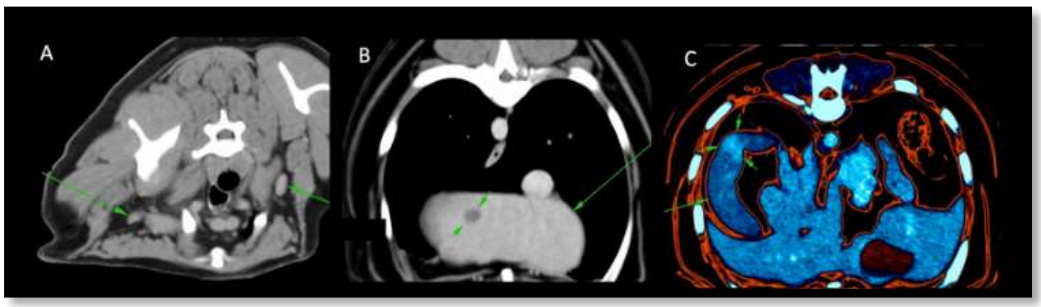

The chromotherapy sessions were restarted, and ozone therapy was suspended from this moment onwards. The fermented *Viscum album* P D3 (Injectcenter®/Iscador®)

was replaced by the fermented *Viscum album* Qu D2 (Injectcenter®/Iscador®) in intravenous applications, three times a week. The remaining protocol was not altered.

The blood count and biochemical measurements performed in September 2020 (Table 1 - Sept-20) were within normal limits, following the same pattern as the exams previously performed. The patient's clinical condition remained stable, with no significant complaints from the owners, despite the knowledge of the tumor evolution. At the beginning of October 2020, the animal started to feel inappetence and discouraged, quickly progressing to difficulty walking with the hind limbs. The clinical signs were compatible with the existing disc protrusion, followed-up in all imaging exams. Conservative treatment was started using acupuncture and physical therapy associated with injectable subcutaneous applications of Arnica D9 (Injectcenter®), one ampoule, twice a day, for 15 days. After this period, there was no clinical improvement, and PCR was performed for *Leishmania infantum*, *Babesia canis*, *Borrelia* sp., *Anaplasma* sp., and *Ehrlichia canis*, all of which were negative. Therefore, the patient was referred for a new imaging exam. The CT was performed on October 03, 2020. The images showed the presence of an amorphous, expansive, infiltrating neoformation with well-defined limits. It was located in the left maxilla, at the level of upper premolars, and invaded the left nasal cavity, in the topography of the ventral nasal meatus, measuring about 4.45 cm in height x 4.20 cm wide x 7.54 cm long (Figures 9A and B). Absence of upper teeth suggestive of being the first and third incisors, right canine, and left premolars (teeth 101, 103, 104, 205, 206, 207, and 208). Bone lysis of the alveolar processes of the left premolar teeth, left maxilla, and palatine process of the left maxilla. The left retropharyngeal lymph node had increased volume, evidenced by an oval, low-uptake, well-delimited nodule, measuring approximately 0.32 cm in diameter. The right retropharyngeal lymph node also presented increased volume. Thorax (Figure 9C) - images suggestive of enlargement of the sternal lymph nodes. A focus of alveolar infiltrate was observed in the left caudal lobe (Figure 9D). The cardiac silhouette, thoracic aorta, and cranial and caudal vena cava were normal. Abdomen - the liver (Figure 9F) presented an oval area with poorly defined limits and low-uptake contrast in the left lateral lobe, approximately 2.50 cm in diameter. There was also an amorphous area with poorly defined limits and heterogeneous contrast uptake, predominantly low-uptake. It was located in the left medial lobe topography and measured approximately 4.1 cm in height x 4.9 cm in width x 5.4cm in length (Figure 9E). The pancreas and adrenal glands were normal. The spleen presented increased

volume, irregular contours, heterogeneous contrast enhancement, and multiple hyper-uptake nodules with poorly defined limits. The largest nodule measured approximately 1.87 cm in diameter and was located in the head of the spleen (Figure 9G). The kidneys, abdominal aorta, caudal vena cava, portal vein, intestinal loops, urinary bladder, and prostate were normal. A well-delimited, oval, isodense, subcutaneous nodule was located in the left ventrolateral region of the cranial abdomen, at the level of the ninth rib, measuring approximately 1.4 cm in diameter. Hyperattenuating content with characteristics of intervertebral disc protrusion between the L7-S1 vertebrae (Figure 10A), central, measuring approximately 207 HU* (Hounsfield Unit), consistent with partially mineralized material from the intervertebral disc, occupying about 90% of the spinal canal, thus compressing the innervations of the spinal cord. Ventral deforming spondylosis was also observed, partially obliterating the neural foramina (Figure 10B). Posterior elements were normal, with no further noteworthy changes.

Figure 9: A and B) Presence of neoformation invading the left nasal cavity in the ventral nasal meatus topography. C) Lung with no apparent changes. D) Focus of alveolar infiltrate in left caudal lobe. E) Nodule in the liver. F and G) Spleen with multiple nodules and a nodule in the head of the spleen.

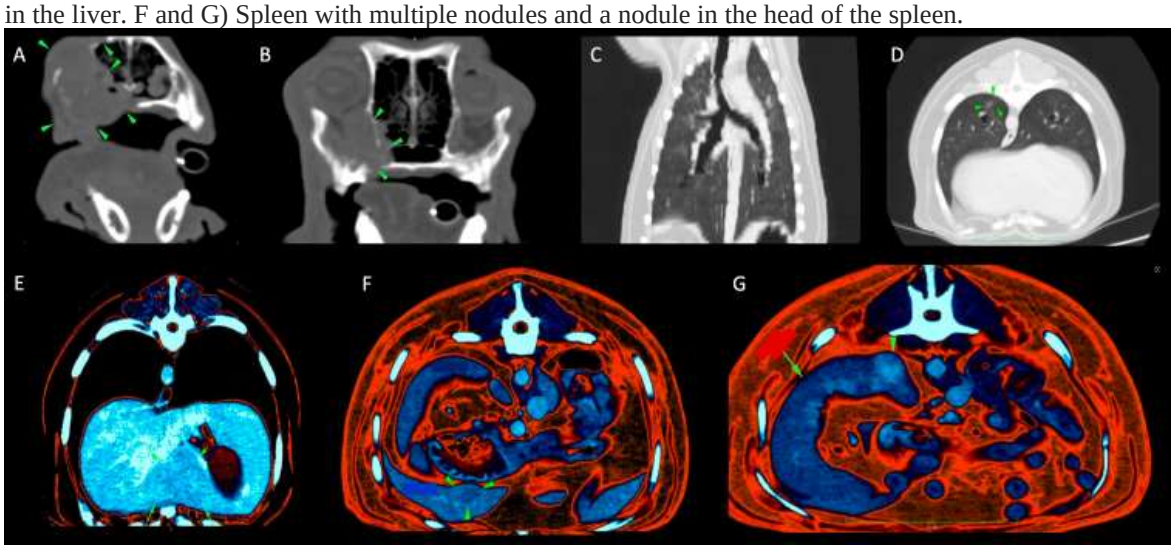

The patient's clinical condition worsened the day after this last exam was performed. He was then referred for admission to an intensive care unit - ICU. The results of the blood count and biochemical measurements performed in early October (Table 1 - 01-Oct-20) indicated an initial picture of anemia, a slight increase in leukocytes, but the most aggravating factor was the development of acute kidney disease. The animal was treated with supportive medication for its current condition for one week. The new blood exams (Table 1 - 07-Oct-20) indicated an unfavorable health state, with a slight

improvement in his condition. The patient was referred to specific assistance at a nephrology hospital to undergo peritoneal dialysis (08-Aug-20), with subsequent return to the ICU. Additional exams were performed after two days (Table 1 - 10-Oct-20), demonstrating worsening of anemia and hematocrit associated with evident thrombocytopenia. A significant improvement in the amount of phosphorus and creatinine was verified. However, the animal died on that day due to a cardiorespiratory arrest.

Figure 10: A) Intervertebral disc protrusion between the L7-S1 vertebrae. B) Intervertebral disc protrusion between the L7-S vertebrae; ventral deforming spondylosis partially obliterating the neural foramina.

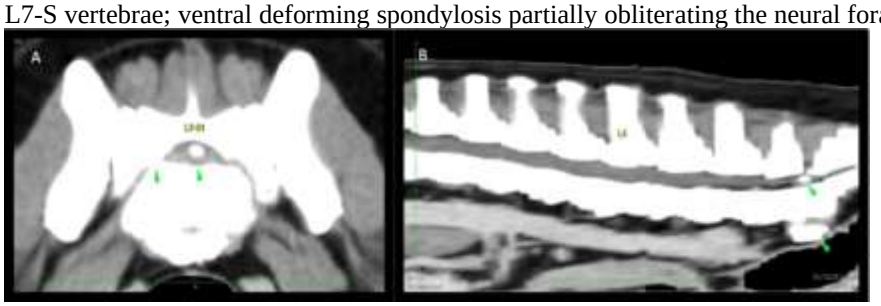

4 DISCUSSION

Fibrosarcoma is more commonly seen in dogs with an average age between 7 and 12 years [5]. Our data corroborate this information presenting a case of a 10-year-old patient that has a breed predisposition to the disease. Fibrosarcomas are tumors that can grow quickly or slowly, depending on the degree of differentiation. The slow-growing form is the more prevalent [5].

Fibrosarcomas are rarely metastatic tumors and occur in percentages lower than 20-25% of cases depending on the histological grade [5]. However, in the present report, possible metastases were identified. The first metastasis was detected in the spleen, and later, another metastasis was found in the liver (Table 2) with no possibility of carrying out the confirmation by histopathological examination.

Treatment for fibrosarcoma is hampered in veterinary and human medicines due to the late diagnosis of the patient, who demonstrates clinical signs in more advanced stages of the disease [14]. The surgical procedure is the treatment of choice considering the low recurrence rate and low metastatic index [15], [16] when a wide surgical margin is provided. The breed, age of the patient, and tumor mass location have little influence on the prognostic, which is closely related to histological characteristics [17]. The rapid growth observed in this report indicated aggressiveness, which could be classified as a

reserved to poor prognosis, given that the maxillectomy procedure was not performed. The animal underwent the first procedure to remove the tumor. On histopathology, it was found that the sample had free vessels and compromised margins. One year after this procedure, a new procedure was performed, but this time, on the contralateral side. No compromised cells were found in the biopsy sample.

Vasconcelos [18] described an oral fibrosarcoma in a 12-year-old female Golden Retriever, weighing 42 Kg. The animal had a mass adhered to the rostral portion of the jaw. It was encapsulated, measured about 5 cm in diameter, and extended cranially to the nasal plane, causing an obstruction. The patient underwent neoadjuvant cytoreductive chemotherapy and bilateral rostral maxillectomy. However, this surgical procedure was extremely radical, and its follow-up was only 30 days. Nevertheless, the case reported in this study contradicts such treatment since it does not have a radical approach or administration of conventional drugs. Additionally, the follow-up period was 24 months, and survival after the initial diagnosis was 27 months (Table 2).

This report showed rapid initial growth of the fibrosarcoma and no clinical symptoms, differing from literature data that cites inappetence and reluctance to move as the primary pain symptoms. Also, the patient did not have pulmonary metastasis, the most common type in fibrosarcoma [5], until the moment of his death. The mass size and location agreed with the literature, which reports a variation from 1 to 15 cm in diameter [2], [5]. The patient was stable after the intervention in November 2018 and had no changes in the initial neoplasm focus until January 2020. Despite the progressive tumor increase after 13 months of the last surgical procedure, the patient had an excellent quality of life. The animal was cheerful throughout the treatment period, totaling 27 months of survival. No changes were recorded in appetite, pain, sleep, and overall disposition during this period, except in the last month. The L7-S1 disc protrusion worsened in his last month of life, reaching 90% compression (Table 2), with no surgery possibility for spinal cord decompression due to the patient's clinical condition. After an imaging exam, the patient died from acute kidney disease due to anesthesia.

The present study corroborates Biegel et al. [19], Klocke et al. [20], and Blostin and Faivre [21], who reported promising results of quality of life associated with longevity of veterinary patients diagnosed with oral fibrosarcoma and treated by the *Viscum album* therapy, whether or not associated with conventional therapy. We can also mention that the patient was benefited from the proposed treatment for other purposes besides cancer treatment, as he had biliary sludge and sediments in the bladder, which

were resolved after the introduction of complementary therapy with no further interventions.

Table 2: Evolution of the lesions relevant to the patient's condition reported throughout the treatment.

	CT 1 - Nov-18	*CT 2 - May-19*	*CT 3 - Aug-19*	*CT 4 - Jan- 20*	*CT 5 - Jul-20*	*CT 6 - Oct-20*
Left Maxilla	Neoformation in the lateral region of the left third premolar tooth, measuring approximately 0.78 cm in height x 0.4 cm in width x 0.5 cm in length	Images suggestive of partial absence of the left maxilla, and teeth 205, 206, 207, and 208	Images suggestive of partial absence of the left maxilla, and teeth 205, 206, 207, and 208	Images suggestive of partial absence of the left maxilla, and teeth 205, 206, 207, and 208	Presence of an oval, expansive, and infiltrative neoformation in the left maxilla at the level of the upper premolars. It invaded the left nasal cavity in the ventral nasal meatus topography and measured about 2.58 cm in height x 2.48 cm in width x 3.30 cm in length. Absence of upper teeth, suggestive of being the first and third right incisors, right canine, and left premolars (teeth 101, 103, 104, 205, 206, 207, and 208). Bone lysis of the alveolar processes of the left premolar teeth, left maxilla, and the palatine process of the left maxilla.	Presence of an expansive and infiltrating neoformation with well-defined limits at the level of the upper premolars. It invaded the left nasal cavity in the ventral nasal meatus topography and measured 4.45 cm in height x 4.20 cm in width x 7.54 cm in length. Absence of upper teeth suggestive of being the first and third incisors, right canine, and left premolars (teeth 101, 103, 104, 205, 206, 207, and 208). Bone lysis of the alveolar processes of the left premolar teeth, left maxilla, and palatine process of the left maxilla.

Left medial retropharyngeal lymph node	***	***	***	Slight increase in volume, regular contours, and heterogeneous contrast enhancement. Presence of an oval, low-uptake, well-delimited nodule, measuring approximately 0.2 cm in diameter.	Slight increase in volume, regular contours, and heterogeneous contrast enhancement. Presence of an oval, low-uptake, well-delimited nodule, measuring approximately 0.2 cm in diameter.	Increased volume. Presence of an oval, low-uptake, well-delimited nodule, measuring about 0.32 cm in diameter. The right retropharyngeal lymph node has increased volume.
Liver	***	Single nodule - 1.1 cm in diameter	Single nodule - 0.68 cm in diameter	Single nodule - 1.18 cm in diameter	Presence of nodule measuring approximately 1.20 cm in height x 1.95 cm in width x 0.98 cm in length	Presence of an oval area with poorly defined limits, low-uptake contrast, located in the left lateral lobe, approximately 2.50 cm in diameter. Nodule in the left lobe, 4.1 cm in height x 4.9 cm in width x 5.4 cm in length.
Gallbladder	Isodense Content	***	***	***	***	***
Spleen	Multiple nodules - the largest with 0.6 cm in diameter	Multiple nodules - the largest with 1.2 cm in diameter	Multiple nodules - the largest with 1.01 cm in diameter	Multiple nodules - the largest with 1.7 cm in diameter	Presence of multiple hyper-uptake nodules, with poorly defined limits, distributed throughout the splenic parenchyma. The largest nodule was located in the head of the spleen and measured approximate	Multiple hyper-uptake nodules, with poorly defined limits, the largest with about 1.87 cm in diameter and located in the head of the spleen

					ly 1.80 cm in diameter.	
Urinary Bladder	Isodense Content	***	***	***	***	***
Bilateral Axillary Lymph Nodes	***	***	***	Increased in size	***	***
Lung	***	***	***	***	***	Alveolar infiltrate focus in left caudal lobe
Column	***	Disc protrusion – L7-S1	Disc protrusion - L7-S1 with 70% compression	Disc protrusion - L7-S1 with 70% compression	Central disc protrusion - L7-S1 with 70% compression	Intervertebral disc protrusion between the L7-S1 vertebrae partially mineralized material from the intervertebral disc, occupying about 90% of the vertebral canal, thus compressing the spinal cord innervations
Left ventrolateral subcutaneous region of the thorax	***	***	***	Nodule with 1.4 cm in diameter	***	***
Left ventrolateral region of the cranial abdomen, at the level of the ninth rib	***	***	***	***	Presence of a subcutaneous, oval, isodense, and well-delimited nodule measuring approximately 1.4 cm in diameter	***

5 CONCLUSION

Conventional cancer treatments for fibrosarcoma do not include the cure or even improve the patients' living conditions. This type of treatment always involves mutilation with the amputation of the affected parts. Conventional medicines are also used, most of

which may cause serious side effects and even lead to the impossibility of following up with the treatment.

Therefore, we emphasize that the best choice would be the association of conventional with complementary therapy, always prioritizing the patient's quality of life. In this context, we showed that the treatments used in this study were well-management and effective in their purpose, improving the patient's quality of life and life expectancy.

DECLARATION OF CONFLICT OF INTEREST

The authors declare that they have no conflict of interest.

REFERENCES

[1] T.L. Gross, P.J. Ihrke, E.J. Walder, V.K. Affolder. Skin Diseases of the Dog and Cat: Clinical and Histopathologic Diagnosis, Roca Press, Sao Paulo, 2009.

[2] E.G. Macewen, B.E. Powers, D. Macy, S.J. Withrow. "Soft tissue sarcomas," in Withrow and MacEwen's small animal clinical oncology, S.J. Withrow and D.M. Vail (eds.), W.B. Saunders, Philadephia, 2012.

[3] N.R. Senthil, R. Chakravarthi, S. Vairamuthu. "Retrospective studies on tumor conditions in dogs over a period of four years (2014-2018)," The Pharma Innovation Journal, 9 (4S), pp. 224-227, 2020.

[4] K. Grüntzig, R. Graf, G. Boo, F. Guscetti, M. Hässig, K.W. Axhausen, S. Fabrikant, M. Welle, D. Meier, G. Folkers, A. Pospischil. "Swiss Canine Cancer Registry 1955-2008: Occurrence of the Most Common Tumour Diagnoses and Influence of Age, Breed, Body Size, Sex and Neutering Status on Tumour Development," Journal of Comparative Pathology, 155(2-3), pp. 156-170, 2016.

[5] M.H. Goldschmidt, M.J. Hendrick. "Tumors of the skin and soft tissues", in Tumors in domestic animals, D.J. Meuten (ed.), Iowa State Press, Philadelphia, 2002.

[6] J.M. Liptak, S.J. Withrow. "Oral tumours," in Small animal clinical oncology, S.J. Withrow & D.M. Vail (eds.), Saunders Elsevier, St Louis, Missouri, 2007.

[7] G.D.L. Nunes, K.D. Filgueira. “Clinical and microscopic findings of fibrosarcoma in the oral cavity of a canine,” Revista de Educação Continuada em Medicina Veterinária e Zootecnia do CRMV-SP, 11 (3), p. 77, 2013.

[8] J.M. Liptak, L.J. Forrest. "Soft tissue sarcomas," in Withrow and MacEwen's small animal clinical oncology, S.J. Withrow and D.M. Vail (eds.), W.B. Saunders, Philadephia, 2012.

[9] I. Mikaelian, T.L. Gross. "Keloidal fibromas and fibrossarcomas in dog," Veterinary Pathology, 39 (1), pp. 149-153, 2002.

[10] S.J. Withrow, J.P. Farese. "Surgical oncology," in Withrow and MacEwen's small animal clinical oncology, S.J. Withrow and D.M. Vail (eds.), W.B. Saunders, Philadephia, 2012.

[11] A.C.V. Valle, L. Lima, L. Bonamin, H. Brunel, A. Barros, A. Carvalho A. "Use of *Viscum album* in the Integrative Treatment of Cholangiocarcinoma in a Dog (*Canis familiaris*) - Case Report," Advances in Complementary & Alternative Medicine, 5(4), pp. 476-481, 2020.

[12] A.C.V. Valle. "In vitro and in vivo evaluation of the ultra-diluted *Viscum album* efficacy and safety", Doctorate dissertation, Catholic University of Brasilia – UCB, Brasilia, DF, Brazil, 2020. 78p. In Portuguese

[13] A.C.V. Valle, A.C. Carvalho. "Ultra-diluted *Viscum album* in the Treatment of Cutaneous Melanoma in a Dog (*Canis familiaris*) – Case Report," Paripex – Indian Journal of Research, 10 (4), pp. 1-4, 2021.

[14] M. Nowak, J.A. Madej, P. Dziegiel. "Correlation between MCM-3 protein expression and grade of malignancy in mammary adenocarcinomas and soft tissues fibrossarcomas in dogs," In Vivo, 23(1), pp. 49-53, 2009.

[15] N. Ehrhart. "Soft-tissue sarcomas in dogs: a review", Journal of American Animal Hospital Association, 41(4), pp. 241-246, 2005.

[16] D. Chase, J. Bray, A. Ide, G. Poltron. "Outcome following removal of canine spindle cell tumours in first opinion practice: 104 cases," Journal of Small Animals Practice, 50(11), pp. 568-574, 2009.

[17] G.K Olgivie, A.S Moore. "Fibrossarcoma in dogs. Managing the veterinary cancer patient: a practice manual," Veterinary Learning Systems Company, Treton, 1995.

[18] M. Vasconcellos. "Oral fibrosarcoma of low histological grade and high biological aggressiveness: case report," PubVet, 12(7), p. 138, 2018.

[19] U. Biegel, K. Ruess-Melzer, P. Klocke. "Orally administered *Viscum album* Quercus dilutions in the therapy of feline fibrosarcoma in cats," Phytomedicine, 18(SVIII), p. 24, 2011.

[20] P. Klocke, U. Biegel, O. Clottu, M. Ramos, V. Gerber, K. Ruess-Melzer. Using *Viscum album* extracts (ISCADOR) for successful management of neoplasms of the skin in horses and cats in consideration of aspects relevant to human medicine. European Journal of Integrative Medicine, 1(1), p. 6, 2008.

[21] R. Blostin, C. Faivre. “Bénéfices du gui fermenté chez le chat aprèsexérèse de fibrosarcome. Résultats d'une étude préliminaire”, Phytothérapie, 6(6), pp. 352-358, 2008. In French.